Journal Pre-proof

Thermal gelation and hardening of whey protein beads for subsequent dehydration and encapsulation using vitrifying sugars

Mackenzie M. Hansen, Valentyn A. Maidannyk, Yrjö H. Roos

PII:	S0260-8774(20)30064-9
DOI:	https://doi.org/10.1016/j.jfoodeng.2020.109966
Reference:	JFOE 109966
To appear in:	*Journal of Food Engineering*
Received Date:	16 August 2019
Accepted Date:	06 February 2020

Please cite this article as: Mackenzie M. Hansen, Valentyn A. Maidannyk, Yrjö H. Roos, Thermal gelation and hardening of whey protein beads for subsequent dehydration and encapsulation using vitrifying sugars, *Journal of Food Engineering* (2020), https://doi.org/10.1016/j.jfoodeng.2020.109966

This is a PDF file of an article that has undergone enhancements after acceptance, such as the addition of a cover page and metadata, and formatting for readability, but it is not yet the definitive version of record. This version will undergo additional copyediting, typesetting and review before it is published in its final form, but we are providing this version to give early visibility of the article. Please note that, during the production process, errors may be discovered which could affect the content, and all legal disclaimers that apply to the journal pertain.

© 2019 Published by Elsevier.

Journal Pre-proof

Thermal gelation and hardening of whey protein beads for subsequent dehydration and encapsulation using vitrifying sugars

Mackenzie M. Hansen[a], Valentyn A. Maidannyk[b], Yrjö H. Roos[a*]

[a]Food Technology, School of Food and Nutritional Sciences, University College Cork, Ireland

[b]Teagasc, Food Research Centre, Moorepark, Fermoy, Co. Cork, P61 C996

[*]Corresponding author:

E-mail address: yrjo.roos@ucc.ie

Mailing address: Room 348

School of Food & Nutritional Sciences

University College Cork

Cork

Ireland

Tel.: +353 21 490 2386

Journal Pre-proof

Journal Pre-proof

Abstract

Solid beads were developed using whey protein isolate (WPI) and sugars for controlled hardening and vitrification of wall materials. A concentrated mixture of WPI and sucrose in water, intended for use as gelling and glass-forming ingredients, respectively, was used to form liquid feeds with varying pH, viscosities, surface tensions, solids contents and compositions. Using a peristaltic pump, feeds flowed continuously through silicon tubing and formed droplets. Rapid solidification occurred when droplets were submerged in heated, stirred oil; beads were harvested for vacuum oven drying. Dispersions were characterized by viscosity and flow testing. Dried beads were characterized for porosity, hardness, diameters, and water activity, and microstructures were analyzed with microscopy. Drop-forming dispersions comprised of 40% WPI with 10% sucrose by mass possessed structure forming and shape retention qualities. Feed composition influenced characteristics of the final product more strongly than processing conditions including heating times and temperatures.

Journal Pre-proof

1.0 Introduction

Bovine whey proteins are a popular choice when aiming to develop new textures, structures, functions, and products in food (Kulmyrzaev et al., 2000). Whey proteins are often utilized for their nutritional contribution as well as wide range of functional properties including foaming, emulsifying, and gelation. Thermal treatment of whey proteins in solution may result in the formation of a gel network, driving the formation of desired food structures. The first step in gel formation from globular proteins is denaturation. Applying heat causes protein conformations to shift and structures unravel, exposing formerly internally oriented hydrophobic groups. In β-lactoglobulin, a free thiol group from Cys_{121} is exposed, promoting its availability to adopt new

Journal Pre-proof

intramolecular and intermolecular linkages (Sawyer, 2003; Nicolai et al., 2011). At high protein concentrations, intermolecular protein-protein interactions between denatured molecules will lead to aggregation, the second step in gel formation (Fennema, 2017). Segments of different protein molecules interacting via hydrophobic interactions, electrostatic interactions, hydrogen bond formation, and disulfide bond formation leads to formation of aggregates. The final step is the formation of the gel network by successive addition of intermolecular bonds (particularly hydrogen-bonds and hydrophobic interactions) between subunits to make up the 3D structure (Kamerzell et al., 2011).

When sugar was included in protein solutions, Lee and Timasheff (1981) reported an unfavorable change in free energy, resulting in sugar molecules being preferentially excluded from the region immediately surrounding proteins. Exclusion occurred due to the higher cohesive force of the sucrose-water system and effect of sucrose to increase surface tension of water (Lee and Timasheff, 1981), as well as a combination of excluded volume effects (sugar molecules are larger than water molecules) and differential interaction effects including protein-dependent interactions comprising of the sum of numerous types of interactions at varied locations on protein surfaces, and protein-independent interactions involving cosolvent molecules at interfaces, depending on cosolvent molecular properties (Baier & McClements, 2001; McClements, 2001, 2002; Semenova et al., 2002). Preferential hydration of proteins results in differences in the composition of the solvent surrounding proteins and that of the bulk solution, thus forming a concentration gradient and applied osmotic stress to protein molecules, where proteins have tendencies to alter their conformations and fold to limit exposure to sugars; some studies suggest that sucrose may be near to fully excluded from protein domains (Lee and Timasheff, 1981; McClements, 2002).

Journal Pre-proof

Journal Pre-proof

In the liquid state, proteins are both protected against unfolding and encouraged to form aggregates after denaturation due to the presence of sucrose in the system. There are two major hypotheses to explain sugars' impact on proteins in the solid state resulting from dehydration: the glass dynamics/ vitrification theory and the water replacement theory (Allison et al., 1999; Chang and Pikal, 2009; Mensink et al., 2017). Both theories require sugar to be in the same amorphous phase as protein in order to impart their effects (Wang et al., 2009), and emphasize the significance of reducing proteins' molecular mobility (Ohtake et al., 2011). It can be presumed, then, that glass formation occurs in the preferentially excluded sucrose fraction of protein-sucrose dispersions.

Most previous studies have been performed under low concentration conditions; our interest is in highly concentrated systems. Schmidt et al. (1984) found that more aggregated, opaque gels would be expected to form at higher protein concentrations and under more severe heating (above 90°C). Additionally, it has been reported that preferential exclusion of sugars increases at higher protein concentrations when sugars and proteins have been combined (He et al., 2011). Regarding relatively dilute protein-solvent-cosolvent systems, McClements (2002) conceded that in practice, it was not possible to completely determine all molecular characteristics of a system due to a large number of differing chemical groups and interactions occurring simultaneously, the highly dynamic nature of the system itself, and limitations of analytical techniques. The challenge to understand the entire body of molecular characteristics of a highly concentrated protein-water-sucrose dispersion is likely even more improbable.

The design and formation of desired food ingredient-based structures, such as biopolymer hydrogels beads from proteins, can be accomplished when the material and functional properties of the components are understood. The injection method of drop formation involves filling

Journal Pre-proof

syringes or tubing with solution, which is then extruded/ injected into a different solution that promotes gelation at selected conditions (Burey et al., 2008; Matalanis et al., 2011; McClements, 2017). The solution drop detachment mechanism is inter-influenced by the physical properties of solution, tip diameter, and solution flow rates (Lee and Chan, 2013), which aid in determining the physiochemical and structural properties of drops such as size, shape, porosity, and hardness (Joye and McClements, 2014; Zhang et al., 2016a, b).

The hypothesis for this study was that a continuous process forming concentrated, liquid feeds into dry, stable particles could be developed. A blend of ice powder and whey protein isolate powder were used for rapid protein hydration during microwave thawing. Rehydrated WPI provided gelation properties of whey proteins to harden beads from a continuous liquid feed with subsequent glass formation of sucrose intended for encapsulation and protection of functional feed components. Our objective was to investigate effects of feed composition and pH on viscosity, surface tension, and bead formation as well as to analyze physicochemical properties of dehydrated beads. Results of this study provide insight into physical behaviors of high solids-concentrated protein dispersions.

Journal Pre-proof

2.0 Materials and Methods

2.1 Materials

Whey Protein Isolate, WPI (Isolac®), used in the present study was supplied by Carbery Food Ingredients (Ballineen, Cork, Ireland). Sunflower oil (Musgrave Excellence™, Musgrave Wholesale Partners, Dublin, Ireland) was purchased from local suppliers. Sucrose (≥ 99.5 GC) of analytical grade was purchased from Sigma-Aldrich, Co. (St. Louis, MO, USA). Citric acid was

Journal Pre-proof

purchased from KB Scientific Ltd. (Cork, Ireland). Ice was utilized as the source of water in experiments.

2.2 Dispersion preparation

A dry blend of sucrose and WPI powder was prepared and stored in a -40°C chest freezer. To prepare liquid feeds, ice at -20°C was weighed and blended in a Duronic BL 1200 stainless steel kitchen blender (4 blades, 1200 W, Duronic, United Kingdom) into a powder with 'ice crush' mode inside a walk-in freezer at -20°C, to prevent melting. The blend of dry ingredients with the powdered ice was mixed together for 15 s prior to thawing in a microwave oven (White manual microwave oven, frequency 2450 MHz, power output 650-700 W, Argos, Ireland) first for 5 min on low settings (120 W, 17% microwave output). The dispersions were mixed by hand to break up any clumps and then heated an additional 1-9 min with the same settings, depending on solids content. Once all ice was melted, dispersions were mixed with a Tefal Infinityforce Ultimate hand blender (ActivFlow Technology with 4 blades, 1000 W, Tefal, Ireland) on 'turbo' mode at a speed setting of '15' for 60 s to break up any larger agglomerates prior to analysis. The pH was measured with the SevenEasy™ probe by Mettler Toledo (Scientific Laboratory Supplies, Nottingham, UK) and adjusted to desired levels with aqueous, 2M citric acid.

2.3 Feed characterization

2.3.1 Viscosity

Viscosity of liquid feed was measured with a Haake RotoVisco 1 (Thermo Scientific, MA, USA). Samples (~13 g) were weighed into a DG43 cup, and a Z41 standard rotor was employed. The water bath surrounding the sample cup was temperature-controlled and held at 20°C. Samples were sheared in a ramp from 0-100 s^{-1} over 3 min, held at 100 s^{-1} for 3 min, then

Journal Pre-proof

ramped back down to 0 s^{-1} within 3 min. A total of 100 measurements were taken over each 3-minute period. Haake RheoWin Job Manager software was used to view and analyze data.

2.3.2 Flow testing

Flow properties of liquid feed at room temperature were measured by pumping through a benchtop, manual control, variable speed, peristaltic pump (120 S/DV; Watson Marlow, Falmouth, England) with silicon tubing of 85 cm length, 2 mm bore, and 1 mm wall thickness (BÜCHI Labortechnik AG, Flawil, Switzerland) at a pump speed of 10 rpm. The time required to deposit 10 mL of liquid feed was measured. Additionally, the number of drops deposited per 1 min was recorded. Mass of 10mL of liquid feed was taken, as well as the average mass of a drop (triplicate measurement). These measured and recorded values allowed for mass flow rates, volume flow rates, liquid feed densities, drop surface tensions, drop diameters, and drop volumes to be calculated.

Density of liquid feed (kg/m^3) was calculated by (1):

$$\frac{mass\ (g)\ of\ 10\ mL\ liquid}{10\ mL\ of\ liquid}$$

Average drop volume (mL) was calculated by (2):

$$\frac{10\ mL\ liquid}{time\ (s)\ to\ deposit\ 10\ mL\ of\ liquid} * \frac{60s\ \ per\ min}{\#\ drops\ per\ min}$$

Mass flow rate (kg/s) was calculated by (3):

$$\frac{mass\ (g)\ of\ 10\ mL\ liquid}{time\ (s)\ to\ deposit\ 10\ mL\ of\ liquid}$$

Volume flow rate (m^3/s) was calculated by (4):

$$\frac{mass\ flow\ rate\ (\frac{kg}{s})}{liquid\ density\ (\frac{kg}{m^3})}$$

Journal Pre-proof

Drop surface tension was calculated with Tate's Law (Worley, 1992) (5):

$$\frac{(Average\ drop\ mass\ (g) * acceleration\ due\ to\ gravity\left[9.8\frac{m}{s^2}\right])}{2\pi * (external\ diameter\ of\ tubing\ tip\ [mm] * correction\ factor\left[\frac{drop\ radius}{(drop\ volume)^{\frac{1}{3}}}\right])}$$

The correction factor in this calculation is in place because the total drop formed at the tip of the outlet tubing does not release, and residual liquid is left on the end of the tube.

Drop diameter was calculated by (6):

$$\left[\frac{(3 * average\ drop\ volume\ [mL])}{4 * \pi}\right]^{\frac{1}{3}} * 2$$

This equation is built off the assumption that drops form a perfectly spherical shape, and thus is derived from the equation for the volume of a sphere:

$$V = \frac{4}{3}\pi r^3$$

and the fact that $diameter = 2 * radius$.

2.4 Drop preparation

Liquid feeds at room temperature were pumped through a peristaltic pump (120 S/DV; Watson Marlow, Falmouth, England) with silicon tubing of 85 cm length, 2 mm bore, and 1 mm wall thickness (BÜCHI Labortechnik AG, Flawil, Switzerland). Pump speed settings of 150-200 RPM were used to fill the tube, then pump speed was set to 10 RPM, forming drops of liquid feed. The outlet tubing was placed between a clamp on a retort stand. For bead formation, a 500 mL glass beaker with a magnetic stir bar was set on a Stuart hotplate and magnetic mixer (Cole-Parmer, Staffordshire, UK), filled with 450 mL of heated sunflower oil. The retort stand was arranged so that the end of the outlet tubing was situated above the surface of the hot oil. Liquid

Journal Pre-proof

feed was pumped through the tubing and dispensed dropwise into the hot oil, being gently stirred with low magnetic agitation by the magnetic stir bar. Drops were allowed to harden in the oil and harvested to dry on absorbent paper before being transferred to Anumbra® glass petri dishes (80 x 15 mm, Scientific Glass Laboratories Ltd., Staffs, UK) for drying. To determine the optimal heating time and temperature conditions to produce beads, drops of the same composition were formed under a range of temperatures and times: at 100°C for 1, 2, 5, and 10 min, and for 2 min at 80, 100, 110, and 120°C.

Glass dishes with beads were placed into a WTB Binder vacuum oven (Binder GmbH, Tuttingen, Germany) at 70°C for 3 h. After drying a_w and diameters were measured prior to packaging in heat-sealed, 12/40 Camplex® Metallized Polyester Laminate packaging (Solventless adhesive laminate of: 12 μm printable polyester film, Camplus® metallized on one side, 40 μm polyethylene film; Camvac Limited, UK). Packages were weighed and placed into an incubator (Cooling Incubator, KBP 6151, Series 6000, Termaks, Bergen, Norway) set at 25°C until testing. Packages were reweighed when removed from the incubator for testing, prior to opening (data not reported.)

A range of formulations of varied solids concentrations and compositions, pH, and viscosities were developed and assessed for their ability to form spherical, solid drops that retained their shape and did not stick to one another (see **Table 1**). Liquid feed dispersions of 35% WPI with 10% sucrose at pH 3.5 and 35% WPI with 15% sucrose at pH 4.0 were not pumpable and thus flow testing was not performed.

Journal Pre-proof

Journal Pre-proof

2.5 Bead characterization

2.5.1 Water activity, a_w

Bead a_w was measured with a water activity meter (4TE, AquaLab, Decagon Devices, Inc., WA, USA) at 20°C before and after drying. Approximately 0.5 g of sample was placed in glass Steriplan dishes (6 mm internal height x 35 mm internal diameter) used as sample cups.

2.5.2 Water content

Fresh bead water content was measured gravimetrically by placing approximately 0.5 g of beads into pre-weighed, glass dishes and recording the mass before placing into a vacuum oven for drying at 70°C for 24 h. Masses were recorded again after drying to obtain the difference in mass due to water loss as well as the sum of total solids plus oil remaining in dry beads.

2.5.3 Drop diameters

Diameters of beads were measured 5 times per sample before and after drying with digital Vernier calipers (0-150 mm; Mitutoyo, Japan), and an average value was reported. Accuracy was not a concern as products measured were not particularly viscoelastic or soft, but had semi-solid structures and held their shape (Lee and Chan, 2013). To compare with calculated values for bead diameters, 3 of the 5 measurements were used.

2.5.4 Hardness

Sample preparation - Beads were removed from storage at 25°C and weighed. Drops were placed in a single layer, covering the bottom area (1520 mm^2) of a transparent, polypropylene sample cup with a yellow screw cap (70 mL, 55 x 44 mm, Starstedt, Australia),

Journal Pre-proof

Journal Pre-proof

samples weights were recorded, and lids were placed on the samples until testing. All samples were prepared for texture analysis in triplicate.

Texture analysis - Beads were tested for hardness with TA-XT2i Texture Analyser (Stable Micro Systems, Surrey, UK). A 35 mm platen was utilized to compress drops 3 mm once contact was made with samples. Compression force was measured, and Texture Expert Exceed software was employed to analyze data.

2.5.5 Density

A Micromeritics AccuPyc II 1340 Gas Pycnometer (Micromeritics Instrument Corporation, GA, USA) was utilized to measure average apparent volume and true density of beads by using Helium gas to 4.5 standard (99.995% purity; Irish Oxygen Company Ltd, Cork, Ireland) as the displacement medium, pumped at a steady rate of 145-172 kPa. A sample cup with 10 cm^3 capacity was partially filled, and each sample was measured 10 times during a single test. AccuPyc II 1340 for Windows software was utilized to run tests and view data reports. A Micromeritics GeoPyc™ 1360 (Micromeritics Instrument Corporation, GA, USA) envelope density analyzer was utilized to measure the average envelope density and volume of samples by combining Micromeritics DryFlo™ displacement material and sample (filling roughly ¼ of the chamber) in a 38.1 mm I.D. chamber and measuring 7 times during a single test. The volumes given from the two tests were utilized to calculate sample porosities. All density testing was completed in duplicate.

Porosity was calculated by: $\frac{Total\ volume - Volume\ of\ solids}{Total\ volume} * 100$ or $\frac{GeoPyc\ volume - AccuPyc\ volume}{GeoPyc\ volume}$

2.5.6 Optical light microscopy

Microscopy observation of dried beads was done using an Olympus BX51 (Olympus Corporation, Tokyo, Japan) light microscope with 20x dry objective lens with polarized light.

Journal Pre-proof

Digital images (TIFF, 8-bit) were taken and captured using Jenoptik C14 Imagic camera. Beads were crushed to produce fragments of smaller sizes that could be imaged.

2.5.7 Confocal laser scanning microscopy

Leica TCS SP5 confocal laser scanning microscope (CLSM; Leica Microsystems CMS GmbH, Wetzlar, Germany) was used for dried beads visualization. Fragments of broken beads were placed onto a glass slide and labeled using a mixture of Fast Green and Nile Red (Auty et al., 2001; Maher et al., 2015). The dye mixture containing Fast Green (aq. 0.01 g/0.1 L) and Nile Red were dissolved in polyethylene glycol 400 g/mol (0.1 g/0.1 L) mixed in a ratio 1:40 of Fast Green to Nile Red, which allowed diffusion of the dye molecules into the particles whilst not influencing the particle morphology and preventing solubilization (Maher et al., 2015). Dual excitation at 488 nm/633 nm was used. The confocal images of drop fragments were taken using 20x oil immersion objective with numerical aperture 0.7 z. Stacks were obtained in order to generate a three-dimensional structure of the particle and to identify surface lipid staining (Maher et al., 2015). Red and Green pseudo-colored pictures (8-bit), 512 x 512 pixels in size, were acquired using a zoom factor of 1-3.

2.5.8 Scanning electron microscopy

Fragments from broken dried beads were attached to double-sided adhesive carbon tabs mounted on scanning electron microscope stubs, and then coated with chromium (K550X, Emitech, Ashford, UK). Scanning electron microscopy images were collected using a Zeiss Supra 40P field emission SEM (Carl Zeiss SMT Ltd., Cambridge, UK) at 2.00 kV. Representative micrographs were taken at 200×, 500×, 1000×, 5000×, and 10000× magnification.

2.6 Statistical analysis

Journal Pre-proof

Journal Pre-proof

All analyses were carried out in triplicate with the exception of envelope and true densities, done in duplicate. The obtained data were analyzed by calculating mean values and standard deviations. Additionally, t-test and analysis of variance (ANOVA; Tukey's HSD test) were performed using R i386 version 3.5.1 (R Foundation for Statistical Computing, Vienna, Austria) on mean values for different samples. The level of significance was determined at $p < 0.05$.

3.0 Results and Discussion

3.1 Feed characterization:

3.1.1 Viscosity

Feed viscosity plays a significant role in drop formation, requiring sufficiently high viscosities to form and retain spherical shapes upon hardening, as competing forces exist between the viscous, surface tension forces of the droplet that must exceed the impact, drag forces from the bath attempting to disrupt shape (Chan et al., 2009). Increasing the concentration of biopolymers in the dispersion is known to increase feed viscosity exponentially (Chan et al., 2009; Matalanis et al., 2011; Lee and Chan, 2013). Highly concentrated WPI dispersions exhibited pseudoplastic flow behavior (data not shown), also observed by Pradipasena and Rha (1977) for β-lactoglobulin above 5% w/w. The apparent viscosity of liquid feeds sheared at 100 s^{-1} increases non-linearly with WPI concentration, with an extreme, significant jump occurring above 30% WPI w/w (**Fig. 1a**), potentially highlighting a critical packing point where particle volume fractions and interactions become sufficiently high to arrest feed dynamics. Above this critical concentration, feed dispersions undergo a transition from fluid-like to more solid-like behavior due to the crowding or jamming of particles' and aggregates' mobility, resulting in the formation of a stress-bearing, interconnected network (Trappe et al., 2001; Coupland, 2014). Our

Journal Pre-proof

results are in agreement with those reported by Alizadehfard and Wiley (1995) and Patocka et al. (2006), who found that WPI dispersions sheared at a fixed rate of 6.45 s^{-1} showed marginally increasing viscosity up to 30% WPI concentration followed by sharp increases. He et al. (2011) reported similar findings, with increases being minimal at lower protein concentrations and the slope of viscosity change significantly increasing at higher protein concentrations when two types of monoclonal antibody proteins were studied. Small shifts in solution conditions, including altered concentration of solutes, can result in the partial unfolding of protein molecules and the exposure of hydrophobic groups. This increases the tendency of protein particles to cluster and form aggregates, as exposed hydrophobic groups are attracted, ultimately increasing the viscosity of the aqueous phase (Song, 2009). Matalanis et al. (2011) explained that increased concentrations of biopolymers increase viscosity until the packing of molecules becomes so tight that a critical packing parameter is reached, above which systems behave more like solids. When protein molecules exceed a critical concentration in a sol, increased entangling and overlap results in increased system viscosity (Coupland, 2014). Crowding results in increased viscosities due to steric repulsion between molecules causing jamming of protein particle movement and ultimately adopting solid-like behavior (Hong et al., 2018). We observed the solid-like behavior of dispersions as feeds that were unable to flow through tubing to form drops.

Sugars increase biopolymer dispersion viscosities (McClements, 2002; Semenova et al., 2002). He et al. (2011) demonstrated that seven different sugars significantly increased viscosity of highly-concentrated protein dispersions. Disaccharides showed stronger effects than monosaccharides when dispersions contained equal amounts of monosaccharide units. Our study showed that feeds of equal protein concentrations exhibited increasing viscosities with increased sucrose concentrations, potentially due to the increase in total system solids as well (**Fig. 1b).**

Journal Pre-proof

Proteins are particles that may exhibit more hydrophilic or hydrophobic behavior, depending on which constituent groups are exposed to the bulk solvent. Globular proteins in their native, folded state are often fairly soluble in water due to their 3D structures having mainly hydrophilic surface groups exposed to water in solution, while the majority of hydrophobic residues are buried within the internal core of the molecule and shielded from interacting with water (Coupland, 2014). The hydrophilic residues exposed to the bulk solvent may contribute to hydrogen bond formation with water molecules. At pH values away from the protein isoelectric point (pI), charged protein molecules repel one another strongly and hydrophobic groups are not exposed. These conditions are unfavorable for the formation of intermolecular interactions and allow protein molecules to exist as separated, suspended particles in water with low solution viscosities (Song, 2009; Coupland, 2014). At pH values near the protein pI, net charges on protein molecules are neutralized and electrostatic interactions are weak. Under these conditions, protein molecules have a stronger tendency to aggregate due to attractive electrostatic forces, reducing solubility. Therefore, altering pH conditions may change the viscosity of biopolymer dispersions, as the volume of electrostatic repulsions and attractive forces between molecules in solution can change with pH (Hong et al., 2018).

Effects of pH of feeds on viscosity are shown in **Figure 1c**. Dispersions comprised of 35% WPI with 10% sucrose showed high viscosities below and up to pH 4, followed by a rapid decrease in viscosity between pH 4 and 4.5, and finally an increasing viscosity with increasing pH above 4.5. Higher pH ranging over 4 to 6.8 showed no significant differences ($p > 0.05$). Our findings were in line with those of Hermansson (1975), who found that increased pH slightly increased viscosities of aqueous whey protein concentrates above the isoelectric point range (pH 4-5). Dissanayake et al. (2013) also reported that whey protein dispersions at pH 4 had higher

Journal Pre-proof

initial viscosities than at pH 5 and 6. Hong et al. (2018) reported that bovine serum albumin (BSA) has a pI of 5.1 and a U-shaped curve for viscosity as a function of pH. BSA solutions with acidic and basic pH were more viscous than BSA solutions at the pI, indicating that monopole-monopole electrostatic repulsions were the dominant factor in solution viscosity and were most reduced at neutral pH.

3.1.2 Flow

The surface tension of feed dispersions strongly determines the mass and size of detached drops, as drops only detach once the gravitational forces pulling down exceed the surface tension forces acting around the circumference of the dripping tip; diameters of drops formed tend to decrease with the surface tension of feeds (Lee and Chan, 2013). Previous studies indicated that surface tension decreased as viscosity and biopolymer concentrations were increased (Chan et al., 2009; Lee and Chan, 2013). Our findings demonstrated that surface tension increased marginally with WPI concentration until there was a significant increase ($p < 0.05$) above 30% w/w WPI (**Fig. 2a**). Sucrose concentrations did not appear to affect surface tension to the same extent observed with WPI (**Fig. 2b**). Proteins are generally more surface-active molecules than sugars, as they contain both hydrophilic and hydrophobic groups and amino acid residues, and can participate in self-assembly as factors such as charges, temperature, or pH are adjusted (Nicolai, 2016). Adjusting the pH of formulations containing 35% WPI with 10 and 15% sucrose showed very similar effects on surface tension as on viscosity, indicating that pH adjustment was not effective for improving drop formation and retention of spherical shapes (data not shown).

While the overall effect of sucrose and protein concentration on surface tension was unexpected (Chan et al., 2009; Lee and Chan, 2013), drop diameters and surface tension had

Journal Pre-proof

high correlation. Higher solids concentrations result in increased intermolecular interactions and may increase the viscosity of fluid systems, resulting in complex fluid behaviors (He et al., 2011; Tro et al., 2014). Additionally, there may have been variations in protein hydration levels in different feed dispersions. A corresponding effect applies to surface tension; liquids containing molecules with stronger and larger numbers of attractive intermolecular forces tend to have higher surface tension values (Tro et al., 2014). WPI dispersions were highly concentrated and as such, it may be inferred that feeds had high levels of intermolecular interactions and thus displayed highly viscous behavior and high surface tensions as well. Another example of increasing viscosities and corresponding increases in surface tension is in water as temperature decreases (Tro et al., 2014).

3.2 Bead characterization

3.2.1 Drop formation and composition

Formulations in **Table 1** include 4 formulations that showed potential for solid beads formation (30% WPI with 20% sucrose, 35% WPI with 15% sucrose at pH 4.5, 40% WPI, and 40% WPI with 10% sucrose). Compositional and water activity data collected from the liquid feeds, fresh beads, and dry beads are provided in **Tables 2, 3, and 4**. Feed dispersions that formed solid beads were comprised of similar total system solids (40-50%) but exhibited a wide range of apparent viscosities (**Table 5**), indicating that viscosity may not be the strongest parameter determining drop forming abilities in this process. Interestingly, all 4 dispersions fell within a narrow range of surface tension values from 0.0016 to 0.0021 N/m, indicating that surface tension was a more significant factor in determining feeds' ability to form solid beads with our process. Two formulations (40% WPI and 40% WPI with 10% sucrose) produced uniform, spherical beads chosen for further characterization.

Journal Pre-proof

Journal Pre-proof

Studies by Kulmyrzaev et al. (2000) and Fitzsimons et al. (2007) showed differential scanning calorimetry (DSC) heating of native WPI gave a broad, endothermic transition between 60 and 90°C with 2 peaks, the more significant around 70-71°C corresponding to β-lactoglobulin denaturation, and the minor peak shoulder at around 60°C representing α-lactalbumin (Ruffin et al., 2014). Knowledge of these temperatures for thermal denaturation allowed the presumption that when liquid drops enter the oil at 100°C they solidify as the whey proteins aggregate and form a gel network. Additionally, drops of the hydrophilic feeds are likely driven to assume compact, spherical conformations within the oil bath to reduce the surface area in contact with the hydrophobic oil. Simultaneous, rapid vaporization of water expands the protein gel, followed by diffusion and dehydration. Heating and evaporation of the water in liquid drops results in droplet expansion, occurring concomitantly with dehydration and gel formation. Expansion can occur due elasticity of the gel network structure, while removal of water from the structure results in pore formation (as seen in **Figs. 7a, b and 8a, d**) and decreased drop densities. Hardening decreases shrinkage and the final volume is dependent on the extent of viscous flow during dehydration. Further dehydration in the vacuum oven transforms the sucrose to form a glass with fragile sucrose membranes on the dry protein. Such conclusion was based on the glass formation properties of sugars in mixes with proteins when glass transition of sucrose occurs above normal ambient temperature at $a_w < 0.2$ (Roos & Drusch, 2015).

Figure 6a depicts the appearance of a 40% WPI, dried product with dispersed oil droplets and the dehydrated protein network spanning the structure. **Fig. 6b,** left shows the structure with the mixture of protein network and oil droplets. **Fig. 6b,** center shows a more magnified view of the mixed protein and oil droplet structures, indicated by the arrows. The left arrow points towards the appearance of the protein network, and the right arrow highlights the oil

Journal Pre-proof

droplets protruding throughout the structure. **Fig. 6b,** right (confocal) shows a number of the tiny oil droplets found in the structure and confirms their identity, as their sizes are of the same magnitude as those in the SEM images. Thermal gelation of whey proteins involves the self-aggregation of protein molecules into the 3D network which entraps water by capillary forces (Chen et al., 2006); as water diffuses out of the structures in this process, it is possible that the same capillary forces responsible for water entrapment may drive oil uptake into the structure of the bead during gelation and hardening (oil droplets dispersion in the structure may be seen in **Figs. 7b, 8b and d, and 9**). The forces driving this oil uptake appear to be strong enough to force the bulk liquid into tiny droplets that fit throughout the structure and could potentially be enhanced by the gentle magnetic stirring of the oil bath (Kornev & Neimark, 2001). Further investigation would be required to determine the mechanism of such oil droplet formation.

3.2.2 Water activity, a_w

The process of drying fresh beads at 70°C for 3 h in the vacuum oven resulted in the reduction of a_w (from ~0.9 (**Table 3**) to ~0.2 (**Table 4**)), resulting in increased microbial stability. In the comparison of thermal treatments of drops, it was found that increased oil temperatures and heating times resulted in reduced a_w values of fresh beads (**Fig. 3a, b**). Results show a decreasing trend in a_w as oil temperature is increased, with a significant reduction ($p < 0.05$) in a_w occurring between 100 and 110°C (from 0.90 to 0.77 a_w, respectively). A similar, decreasing trend in a_w is observed with increased heating times, with a significant reduction ($p < 0.05$) in a_w occurring between 2 and 5 min of heating (from 0.90 to 0.84 a_w, respectively). Apparently heating time and oil temperature determine the extent of drying, as shown by reduced water contents and water activities.

3.2.3 Drop diameter

Journal Pre-proof

Diameters were measured for beads made from 40% WPI, 40% WPI with 10% sucrose, and 30% WPI with 20% sucrose. Beads obtained from 35% WPI with 15% sucrose at pH 4.5 were not spherical in shape (data not reported). Our results indicated that upon drying, significant shrinkage (as obtained from bead diameters; $p < 0.05$) occurred in the beads made from 40% WPI (from 5.06 fresh to 4.50 mm dried), while beads containing sucrose did not experience shrinkage. This was likely due to the formation of sucrose glass upon drying, preventing further shrinking by stabilizing the protein network structure.

Chan et al. (2009) reported that drops formed from calcium-alginate by dripping sometimes have smaller size than predicted, possibly due to shrinkage experienced in gelling solutions. Our beads produced with 40% WPI had larger fresh diameters than predicted with Equation 6, with the 40% WPI products having significantly larger ($p < 0.05$) diameters than predicted (5.06 and 4.79 mm, respectively). While all beads were observed to show expansion behaviors of the gel networks within the heated oil, it would appear that beads without sucrose underwent more extensive expansion. Feeds containing 40% WPI with 10% sucrose had significantly higher ($p < 0.05$) viscosity compared to those with 40% WPI (1.73 and 0.51 Pa*s, respectively) (**Fig. 1b**); as a result of its higher viscosity, 40% WPI with 10% sucrose beads may have undergone expansion to a lesser extent upon heating. Additionally, feeds with 40% WPI and 10% sucrose contained less water than 40% WPI feeds and thus underwent less drying. Corresponding results would be expected for the beads comprised of 30% WPI with 20% sucrose, but the data showed a significant reduction ($p < 0.05$) in drop diameters compared to predicted values (only 2.19 mm fresh compared to predicted 4.39 mm; data not reported). That may be due to the reduced protein content causing weakness in the typically strong forces of self-assembly imparted by high (40% w/w) concentrations of protein within the feed drops, which

Journal Pre-proof

Journal Pre-proof

were overcome by the drag forces upon impact with the oil as well as the magnetic stir bar, thus causing the observed breaking of drop structures within the oil bath. The diameters of 40% WPI with 10% sucrose drops were only slightly larger than predicted and not statistically significant, indicating that calculations used to predict drop diameters were accurate.

Drop diameters were also measured to compare thermal treatments of beads and used to calculate bead volumes (**Fig. 4)**. Results show a relationship between decreasing bead volumes and increasing heating times, with a significant reduction ($p < 0.05$) in bead volume occurring between 5 and 10 min of heating (from 83 to 53 mm^3). Decreasing volumes of beads with increasing heating times could be a result of more extensive dehydration occurring within the drops, as confirmed by a_w data, causing further shrinking as more water was lost and structure hardening occurred. Products formed at increasing temperatures were more irregular in morphology and structures were broken, therefore diameters could not be measured.

3.2.4 Hardness

The hardness of dried beads formed by 40% WPI and 40% WPI with 10% sucrose were compared. Hardness was shown to be less with 10% w/w sucrose (from 232 to 155 N), likely due to the formation of a sucrose glass upon drying; **Fig. 7b** shows that the gel structure is largely not visible in dried beads, and it is assumed that much of the gel network may have the smooth, amorphous sucrose glass form around it. When injection methods have been employed to extrude biopolymer solutions containing multiple components, it is possible to form particles with heterogeneous, dispersion-type internal structures where one component may be dispersed within the other (Matalanis et al., 2011). This describes what our data suggests is happening within bead structures, as it appears that the protein phase is independent and forms a gel that is surrounded by the protective, smooth, glassy matrix after dehydration. The presence of glass may cause the

Journal Pre-proof

product to be more fragile by breaking up regions of dense protein-protein interactions with brittle glass, potentially weakening the otherwise dense protein gel network that would form if no sucrose were present. **Figures 7a, 8a, b, and c, and 9 all** depict the glass that forms upon drying, and the clouded appearance of some pieces may be due to the dried, aggregated protein network dispersed throughout or located at the glassy interface. A study by Al-Marhoobi and Kasapis (2005) of concentrated dispersions of gelatin with sugar as a co-solvent indicated that sugars were preferentially excluded from the protein region, with TEM analysis confirming the presence of separate sugar- and protein-rich phases in the product rather than homogeneous mixtures. They reported that the presence of sugars promoted protein association in their system, giving high network strength retention.

In the comparison of thermal treatments of beads, it was found that the hardness of fresh beads increased linearly with heating time (**Fig. 5**). The irregular morphologies and broken nature of beads formed with varied oil temperatures prevented the samples from being measured for hardness, as uniform beads were critical for accuracy of comparisons. Overall, large variations in hardness were recorded, potentially due to the nature of the products as well as the test involving multiple beads per single measurement. Testing of multiple products at once was determined important in describing the products overall, with inherent variability better accounted for.

3.2.5 Densities and porosity

The total volume and true densities of dried beads formed by 40% WPI and 40% WPI with 10% sucrose were measured and used to calculate average total volume and average solids volume in order to calculate porosity. Porosity was not significantly ($p > 0.05$) different for beads prepared from feeds containing 40% WPI and 40% WPI with 10% sucrose. Water

Journal Pre-proof

dehydrates out of structures containing only WPI and leaves pores in the structure, as can be seen in **Figures 7a, and 8 a, c, and d** with rounded cavities throughout the fragments. Structures containing sucrose experience some dehydration and loss of water, but likely remain more fluid and may experience slightly more collapse as the protein network may be diluted by sugars present. These concentrated sucrose solutions form a glassy structure when oven dried, slightly reducing total unoccupied space in the structure as sucrose molecules are sterically larger than water. This is visualized in **Figure 7b**, where smooth, fractured edges highlighted in the images tend to have relatively rounded edges, indicating that sucrose glass formed within the pores left behind from water drying from the product.

In the comparison of thermal treatments of beads composed of 40% WPI with 10% sucrose, it was found that there was no significant variation in porosity of beads with increased heating (**Table 6**). This may indicate that feed composition may more strongly determine drop porosity than processing conditions.

3.2.6 Microscopy

Combinations of optical light-, confocal laser scanning-, and scanning electron microscope images of fractured beads aided in demonstrating the porous, oil-embedded, aggregated protein network structures produced by feeds containing 40% WPI and indicated the presence of a glassy structure in samples containing sucrose.

Fig. 8 a-d are confocal images for 40% WPI with 10% sucrose, and aid in discerning the 'layers' of the structure of the fractured material. Image 'A' highlights proteins in bright red, while other components have darker color. The broken, glassy, translucent structure appears in the image, either embedded with red protein particles or populated with proteins at the glassy surface, and having a round cavity carved into its side, indicative of a broken porous structure.

Journal Pre-proof

Image ‘B’ highlights oil in bright green, with other components having a darker color. It is apparent that the glassy structure is covered with oil droplets, as oil is known to be dispersed throughout the 3D structure based on videos comprised of ‘stacked’ confocal images taken at different depths. Images ‘C’ and ‘D’ also aid in demonstrating the porous structure of the beads as well as the presence of a glassy matrix, protein network, and oil droplets in the structure. Image ‘C’ highlights proteins in bright red and other components with darker hues. A glassy, fractured piece of the structure is at the center of the image in the shape of a cavity, indicative of the presence of a pore in the 3D structure, and an oil droplet (confirmed by image ‘D,’ highlighting oil in bright green) directly at its center. The dark areas of the glassy structures may be sucrose, while the bright red parts lining the pore shows the presence of the protein network. Image ‘D’ shows a dispersion of small oil droplets along the glassy pore. The dark background of the glassy portion indicates the presence of sucrose.

Fig. 9 is a confocal image of the 40% WPI with 10% sucrose beads and a good example of the protein- and oil-highlighted images being layered to give an idea of overall structure composition. Fat appears as bright green, proteins are bright red, and other components (mainly sucrose in this case) are darker. Translucent, glassy fragments are present in the image, with protein scattered throughout, as well as oil droplets dispersed throughout the structure.

Journal Pre-proof

4.0 Conclusions

We report a full process design for simple solidification of liquid dispersions (in an oil bath at 100°C for 2 min) and a structure-forming formulation (40% WPI with 10% sucrose) used further to vitrify; apparent bulk oil inclusion and its emulsification into small drops throughout the structure is demonstrated. This study presents a potential process to make foods with

Journal Pre-proof

entrapped flavors or actives, including emulsion droplets. The process may be a novel alternative to drying or extrusion that is simple, economic, and effective.

Future work is necessary to expand our understanding of the physical properties of feed dispersions including thermal properties and physical states of final beads, to adapt the process to form beads containing active ingredients, and to determine the protectant abilities of wall components and the location of active ingredients in the matrix. A major challenge when aiming to encapsulate bioactive ingredients is the retention of the active throughout the process in order to obtain final materials in which the actives are still accessible. Similar to spray drying, the process presented forms beads capable of containing bioactives that are not expected to suffer exposure to high temperatures; evaporation of water from the structures keeps beads at low temperatures, and the oil temperature is primarily a measure of energy input.

Acknowledgements

This research was supported by funding provided by the Lauritzson Foundation in the form of the Lauritzson Research Scholarship, through the College of Science, Engineering and Food Science (SEFS) at University College Cork. The authors would like to thank the anonymous reviewers and Journal Editor for thorough reading of the manuscript and helpful comments for revision.

Declaration of Competing Interest

The authors hereby declare no conflict of interest.

Journal Pre-proof

Journal Pre-proof

References

Alizadehfard, M. R., & Wiley, D. E. (1995). Viscosity of Whey Protein Solutions . *Iranian Journal of Polymer Science and Technology*, *4*(2), 126–133.

Allison, S. D., Chang, B., Randolph, T. W., & Carpenter, J. F. (1999). Hydrogen Bonding between Sugar and Protein Is Responsible for Inhibition of Dehydration-Induced Protein Unfolding. *Archives of Biochemistry and Biophysics*, *365*(2), 289–298. https://doi.org/10.1006/abbi.1999.1175

Al-Marhoobi, I. M., & Kasapis, S. (2005). Further evidence of the changing nature of biopolymer networks in the presence of sugar. *Carbohydrate Research*, *340*(4), 771–774. https://doi.org/10.1016/j.carres.2004.12.018

Auty, M. A. E., Twomey, M., Guinee, T. P., & Mulvihill, D. M. (2001). Development and application of confocal scanning laser microscopy methods for studying the distribution of fat and protein in selected dairy products. *Journal of Dairy Research*, *68*(03). https://doi.org/10.1017/S0022029901004873

Baier, S., & McClements, D. J. (2001). Impact of Preferential Interactions on Thermal Stability and Gelation of Bovine Serum Albumin in Aqueous Sucrose Solutions. *Journal of Agricultural and Food Chemistry*, *49*(5), 2600–2608. https://doi.org/10.1021/jf001096j

Burey, P., Bhandari, B. R., Howes, T., & Gidley, M. J. (2008). Hydrocolloid Gel Particles: Formation, Characterization, and Application. *Critical Reviews in Food Science and Nutrition*, *48*(5), 361–377. https://doi.org/10.1080/10408390701347801

Chan, E.-S., Lee, B.-B., Ravindra, P., & Poncelet, D. (2009). Prediction models for shape and size of ca-alginate macrobeads produced through extrusion–dripping method. *Journal of Colloid and Interface Science*, *338*(1), 63–72. https://doi.org/10.1016/j.jcis.2009.05.027

Journal Pre-proof

Journal Pre-proof

Chang, L. (Lucy), & Pikal, M. J. (2009). Mechanisms of protein stabilization in the solid state. *Journal of Pharmaceutical Sciences*, *98*(9), 2886–2908. https://doi.org/10.1002/jps.21825

Chen, L., Remondetto, G. E., & Subirade, M. (2006). Food protein-based materials as nutraceutical delivery systems. *Trends in Food Science & Technology*, *17*(5), 272–283. https://doi.org/10.1016/j.tifs.2005.12.011

Coupland, J. N. (2014). *An Introduction to the Physical Chemistry of Food* (illustrated). Springer.

Dissanayake, M., Ramchandran, L., & Vasiljevic, T. (2013). Influence of pH and protein concentration on rheological properties of whey protein dispersions. *International Food Research Journal*, *20*(5), 2167.

Fennema, O. R. (2017). *Fennema's Food Chemistry* (S. Damodaran & K. L. Parkin, Eds.; 5th ed.). CRC Press Taylor & Francis Group.

Fitzsimons, S. M., Mulvihill, D. M., & Morris, E. R. (2007). Denaturation and aggregation processes in thermal gelation of whey proteins resolved by differential scanning calorimetry. *Food Hydrocolloids*, *21*(4), 638–644. https://doi.org/10.1016/j.foodhyd.2006.07.007

He, F., Woods, C. E., Litowski, J. R., Roschen, L. A., Gadgil, H. S., Razinkov, V. I., & Kerwin, B. A. (2011). Effect of Sugar Molecules on the Viscosity of High Concentration Monoclonal Antibody Solutions. *Pharmaceutical Research*, *28*(7), 1552–1560. https://doi.org/10.1007/s11095-011-0388-7

Hermansson, A.-M. (1975). Functional properties of proteins for foods-flow properties. *Journal of Texture Studies*, *5*(4), 425–439.

Journal Pre-proof

Journal Pre-proof

Hong, T., Iwashita, K., & Shiraki, K. (2018). Viscosity Control of Protein Solution by Small Solutes: A Review. *Current Protein & Peptide Science*, *19*(8), 746–758. https://doi.org/10.2174/1389203719666171213114919

Joye, I. J., & McClements, D. J. (2014). Biopolymer-based nanoparticles and microparticles: Fabrication, characterization, and application. *Current Opinion in Colloid & Interface Science*, *19*(5), 417–427. https://doi.org/10.1016/j.cocis.2014.07.002

Kamerzell, T. J., Esfandiary, R., Joshi, S. B., Middaugh, C. R., & Volkin, D. B. (2011). Protein–excipient interactions: Mechanisms and biophysical characterization applied to protein formulation development. *Advanced Drug Delivery Reviews*, *63*(13), 1118–1159. https://doi.org/10.1016/j.addr.2011.07.006

Kornev, K. G., & Neimark, A. V. (2001). Spontaneous Penetration of Liquids into Capillaries and Porous Membranes Revisited. *Journal of Colloid and Interface Science*, *235*(1), 101–113. https://doi.org/10.1006/jcis.2000.7347

Kulmyrzaev, A., Bryant, C., & McClements, D. J. (2000). Influence of Sucrose on the Thermal Denaturation, Gelation, and Emulsion Stabilization of Whey Proteins. *Journal of Agricultural and Food Chemistry*, *48*(5), 1593–1597. https://doi.org/10.1021/jf9911949

Lee, B. B., & Chan, E. S. (2013). Size and Shape of Calcium Alginate Beads Produced by Extrusion Dripping. *Chemical Engineering & Technology*, *36*(10), 1627–1642. https://doi.org/10.1002/ceat.201300230

Lee, J. C., & Timasheff, S. N. (1981). The stabilization of proteins by sucrose. *Journal of Biological Chemistry*, *256*(14), 7193–7201.

Journal Pre-proof

Journal Pre-proof

Maher, P. G., Auty, M. A. E., Roos, Y. H., Zychowski, L. M., & Fenelon, M. A. (2015). Microstructure and lactose crystallization properties in spray dried nanoemulsions. *Food Structure*, *3*, 1–11. https://doi.org/10.1016/j.foostr.2014.10.001

Matalanis, A., Jones, O. G., & McClements, D. J. (2011). Structured biopolymer-based delivery systems for encapsulation, protection, and release of lipophilic compounds. *Food Hydrocolloids*, *25*(8), 1865–1880. https://doi.org/10.1016/j.foodhyd.2011.04.014

McClements, D. J. (2001). Estimation of steric exclusion and differential interaction contributions to protein transfer free energies in aqueous cosolvent solutions. *Food Hydrocolloids*, *15*(4–6), 355–363. https://doi.org/10.1016/S0268-005X(01)00045-5

McClements, D. J. (2002). Modulation of Globular Protein Functionality by Weakly Interacting Cosolvents. *Critical Reviews in Food Science and Nutrition*, *42*(5), 417–471. https://doi.org/10.1080/20024091054210

McClements, D. J. (2017). Recent progress in hydrogel delivery systems for improving nutraceutical bioavailability. *Food Hydrocolloids*, *68*, 238–245. https://doi.org/10.1016/j.foodhyd.2016.05.037

Mensink, M. A., Frijlink, H. W., van der Voort Maarschalk, K., & Hinrichs, W. L. J. (2017). How sugars protect proteins in the solid state and during drying (review): Mechanisms of stabilization in relation to stress conditions. *European Journal of Pharmaceutics and Biopharmaceutics*, *114*, 288–295. https://doi.org/10.1016/j.ejpb.2017.01.024

Nicolai, T. (2016). Formation and functionality of self-assembled whey protein microgels. *Colloids and Surfaces B: Biointerfaces*, *137*, 32–38. https://doi.org/10.1016/j.colsurfb.2015.05.055

Journal Pre-proof

Journal Pre-proof

Nicolai, T., Britten, M., & Schmitt, C. (2011). β-Lactoglobulin and WPI aggregates: Formation, structure and applications. *Food Hydrocolloids*, *25*(8), 1945–1962. https://doi.org/10.1016/j.foodhyd.2011.02.006

Ohtake, S., Kita, Y., & Arakawa, T. (2011). Interactions of formulation excipients with proteins in solution and in the dried state. *Advanced Drug Delivery Reviews*, *63*(13), 1053–1073. https://doi.org/10.1016/j.addr.2011.06.011

Patocka, G., Cervenkova, R., Narine, S., & Jelen, P. (2006). Rheological behaviour of dairy products as affected by soluble whey protein isolate. *International Dairy Journal*, *16*(5), 399–405. https://doi.org/10.1016/j.idairyj.2005.05.010

Pradipasena, P., & Rha, C. (1977). PSEUDOPLASTIC AND RHEOPECTIC PROPERTIES OF A GLOBULAR PROTEIN (β-LACTOGLOBULIN) SOLUTION1. *Journal of Texture Studies*, *8*(3), 311–325. https://doi.org/10.1111/j.1745-4603.1977.tb01184.x

Ruffin, E., Schmit, T., Lafitte, G., Dollat, J.-M., & Chambin, O. (2014). The impact of whey protein preheating on the properties of emulsion gel bead. *Food Chemistry*, *151*, 324–332. https://doi.org/10.1016/j.foodchem.2013.11.071

Sawyer, L. (2003). β-Lactoglobulin. In P. F. Fox & P. L. H. McSweeney (Eds.), *Advanced Dairy Chemistry: Vol. 1: Proteins* (3rd ed., pp. 319–386). Springer.

Schmidt, R. H., Packard, V. S., & Morris, H. A. (1984). Effect of processing on whey protein functionality. *Journal of Dairy Science*, *67*(11), 2723–2733.

Semenova, M. G., Antipova, A. S., & Belyakova, L. E. (2002). Food protein interactions in sugar solutions. *Current Opinion in Colloid & Interface Science*, *7*(5–6), 438–444.

Journal Pre-proof

Journal Pre-proof

Trappe, V., Prasad, V., Cipelletti, L., Segre, P. N., & Weitz, D. A. (2001). Jamming phase diagram for attractive particles. *Nature*, *411*(6839), 772–775. https://doi.org/10.1038/35081021

Tro, N. J., Fridgen, T. D., & Shaw, L. (2014). *Chemistry: A Molecular Approach*. Pearson Canada.

Wang, B., Tchessalov, S., Warne, N. W., & Pikal, M. J. (2009). Impact of sucrose level on storage stability of proteins in freeze-dried solids: I. correlation of protein–sugar interaction with native structure preservation. *Journal of Pharmaceutical Sciences*, *98*(9), 3131–3144. https://doi.org/10.1002/jps.21621

Worley, J. D. (1992). Capillary radius and surface tensions. Using calculations based on Tate's law. *Journal of Chemical Education*, *69*(8), 678.

Zhang, Z., Zhang, R., & McClements, D. J. (2016). Encapsulation of β-carotene in alginate-based hydrogel beads: Impact on physicochemical stability and bioaccessibility. *Food Hydrocolloids*, *61*, 1–10. https://doi.org/10.1016/j.foodhyd.2016.04.036

Zhang, Z., Zhang, R., Zou, L., Chen, L., Ahmed, Y., Al Bishri, W., Balamash, K., & McClements, D. J. (2016). Encapsulation of curcumin in polysaccharide-based hydrogel beads: Impact of bead type on lipid digestion and curcumin bioaccessibility. *Food Hydrocolloids*, *58*, 160–170. https://doi.org/10.1016/j.foodhyd.2016.02.036

Journal Pre-proof

Journal Pre-proof

Declaration of Competing Interest

The authors hereby declare no conflict of interest.

Please note the following:

- All authors have participated in (a) conception and design, or analysis and interpretation of the data; (b) drafting the article or revising it critically for important intellectual content; and (c) approval of the final version.
- This manuscript is not under review at another journal or other publishing venue.
- The authors have no affiliation with any organization with a direct or indirect financial interest in the subject matter discussed in the manuscript

Journal Pre-proof

Journal Pre-proof

Mackenzie M. Hansen: Conceptualization, Methodology, Validation, Formal analysis, Investigation, Resources, Writing- Original Draft, Writing- Review & Editing, Visualization, Project administration, Funding acquisition

Valentyn A. Maidannyk: Investigation, Resources, Writing- Original Draft

Yrjö H. Roos: Conceptualization, Resources, Writing- Review & Editing, Visualization, Supervision, Funding acquisition

Journal Pre-proof

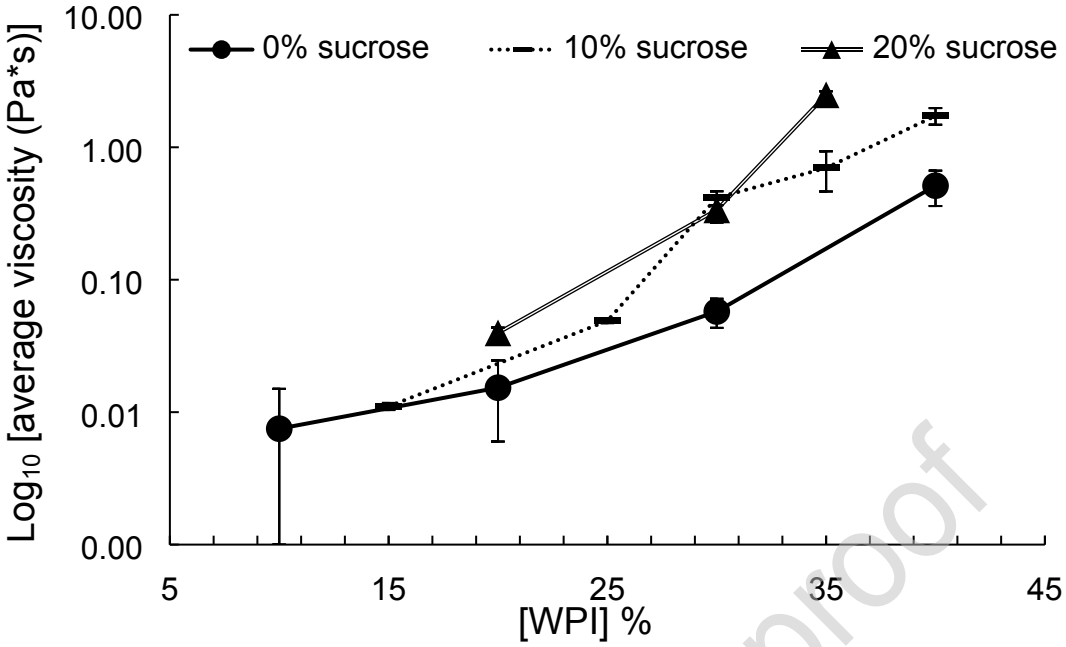

Figure 1a. Effect of protein concentration (%) in feeds containing 0, 10, and 20% sucrose on the apparent viscosity at 100 s^{-1}; n = 3. Lines are for guiding purposes only.

Journal Pre-proof

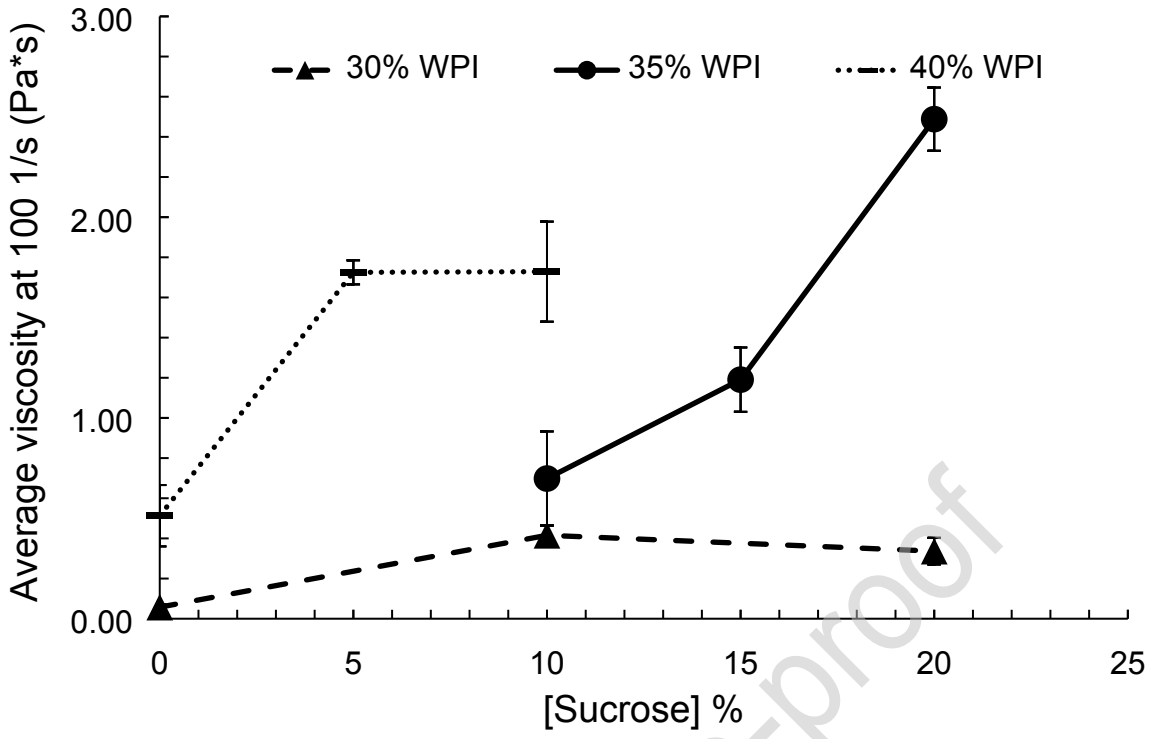

Figure 1b. Effect of sucrose concentration (%) in feeds containing 30, 35, and 40% WPI on apparent viscosity at 100 s^{-1}; n = 3. Lines are for guiding purposes only.

Journal Pre-proof

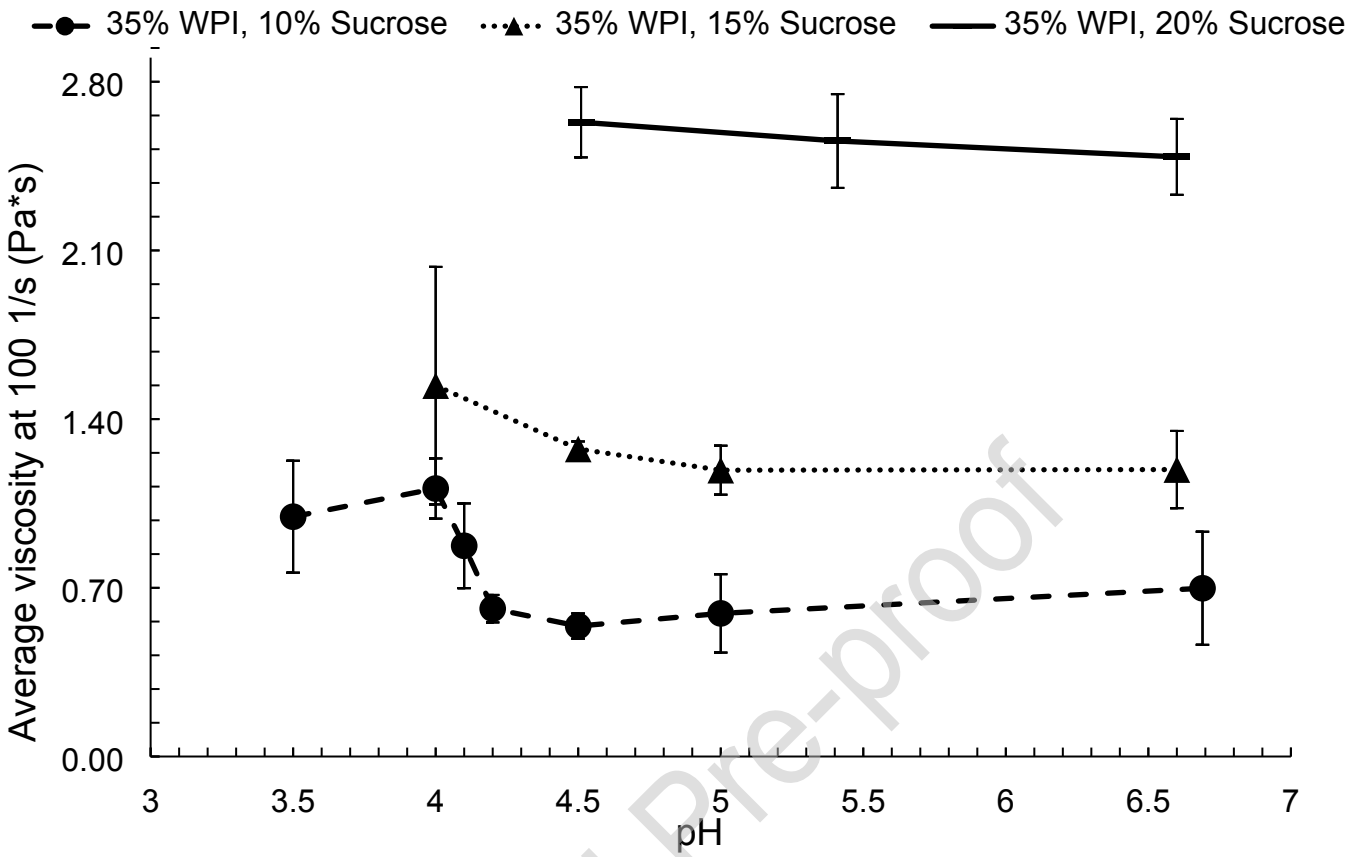

Figure 1c. Effect of pH in feeds containing 35% WPI with 10%, 15%, and 20% sucrose on apparent viscosity at 100 s^{-1}; n = 3. Lines are for guiding purposes only.

Journal Pre-proof

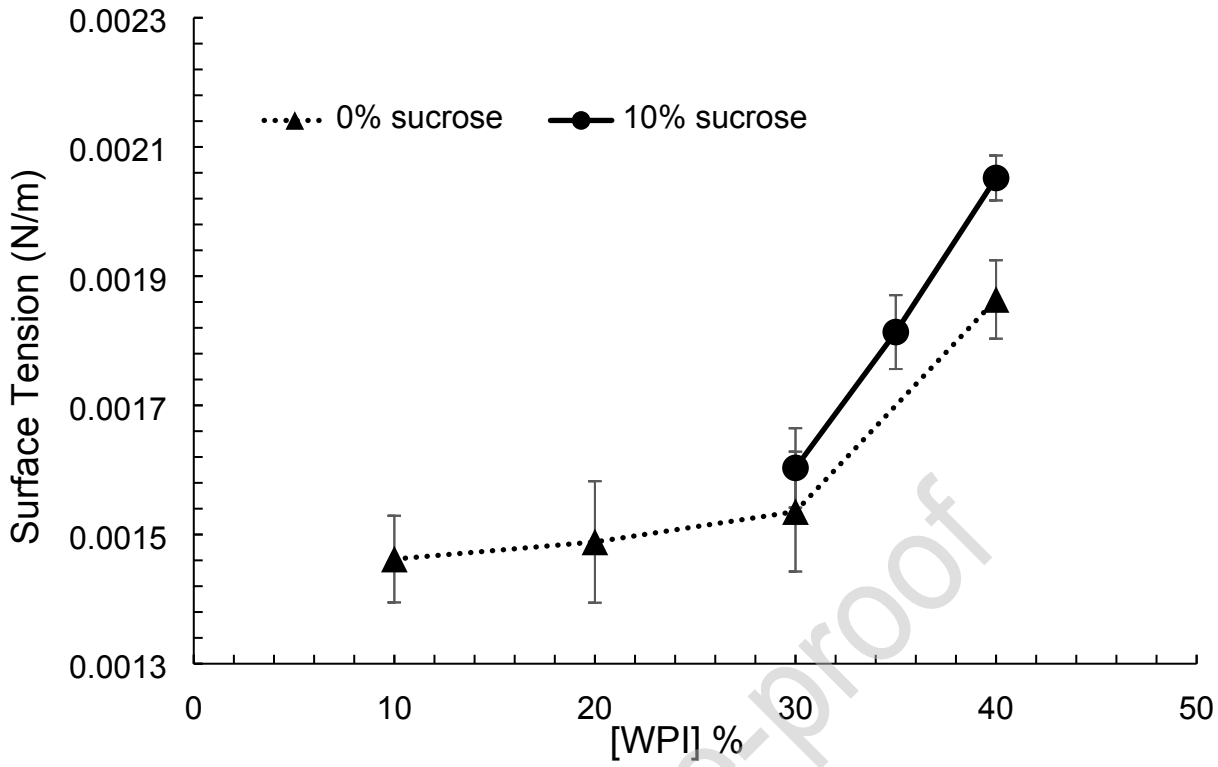

Figure 2a. Effect of WPI concentration (%) in feeds containing 0 and 10% sucrose on calculated surface tension in N/m; n = 3. Lines are for guiding purposes only.

Journal Pre-proof

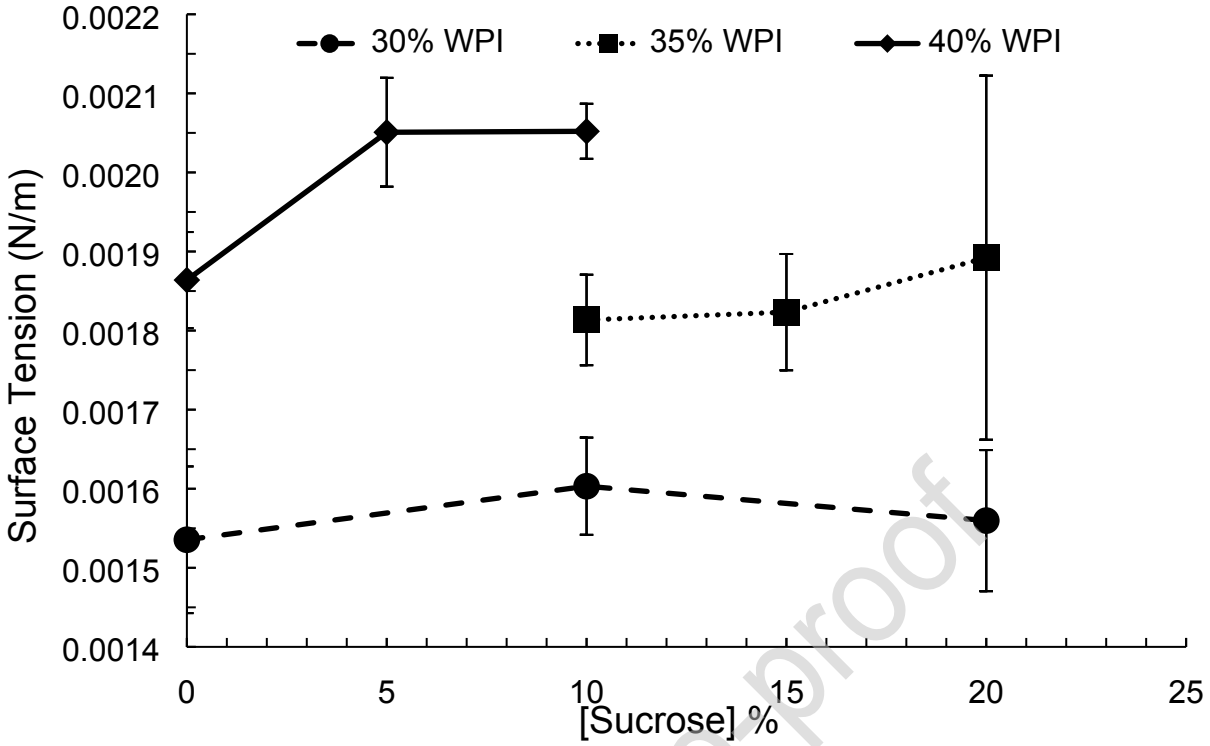

Figure 2b. Effect of sucrose concentration (%) in feeds containing 30, 35, and 40% WPI on calculated surface tension; n = 3. Lines are for guiding purposes only.

Journal Pre-proof

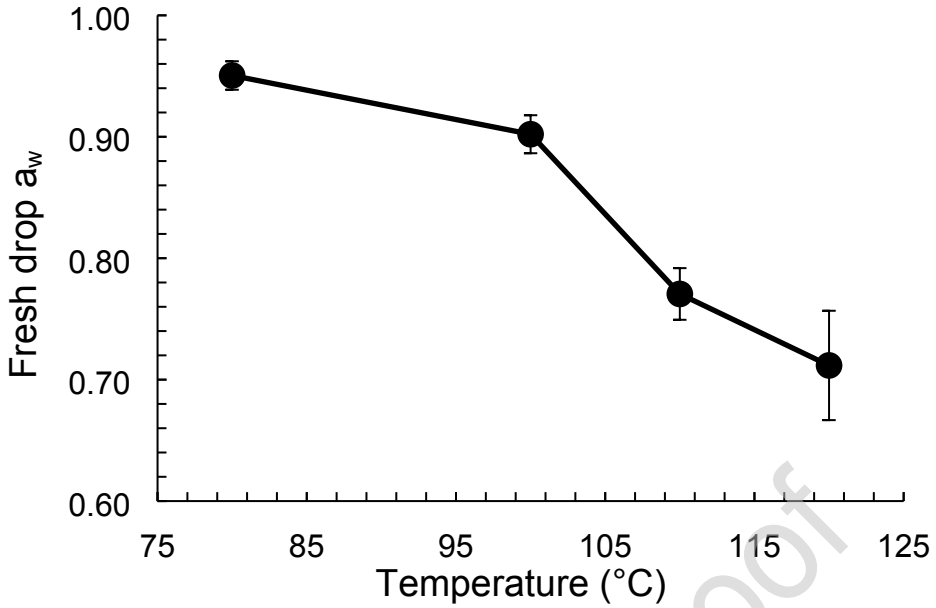

Figure 3a. Effect of oil temperature (°C) on dehydration shown by a_w of fresh drops comprised of 40% WPI with 10% sucrose for 2 min; n = 3. Lines are for guiding purposes only.

Journal Pre-proof

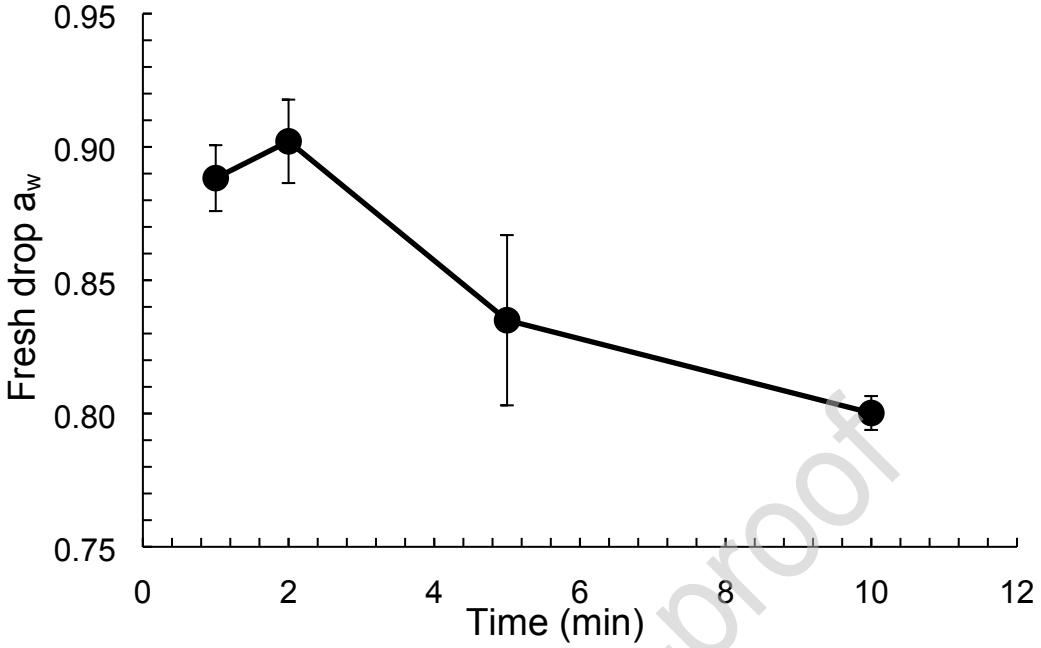

Figure 3b. Effect of heating time (min) at 100°C on dehydration shown by a_w of fresh drops comprised of 40% WPI with 10% sucrose; n = 3. Lines are for guiding purposes only.

Journal Pre-proof

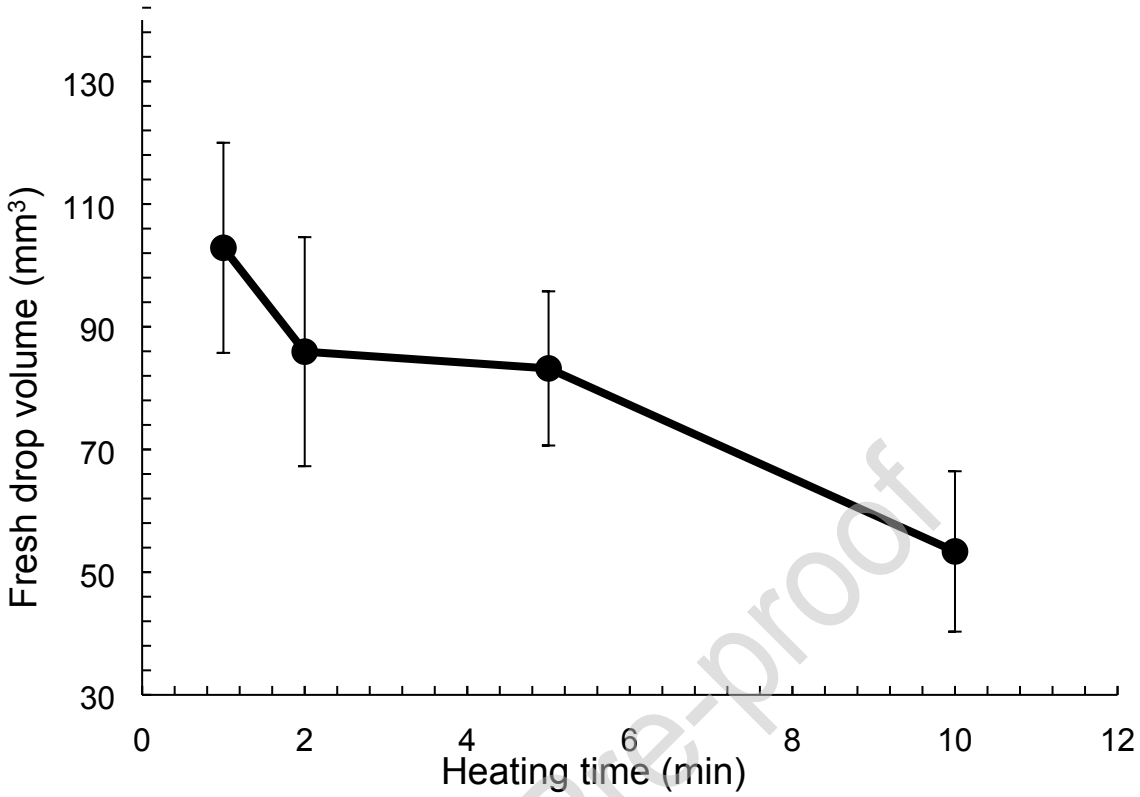

Figure 4. Effect of dehydration shown by heating time (min) at 100°C on the volume (mm^3) of drops comprised of 40% WPI with 10% sucrose; n = 3. Lines are for guiding purposes only.

Journal Pre-proof

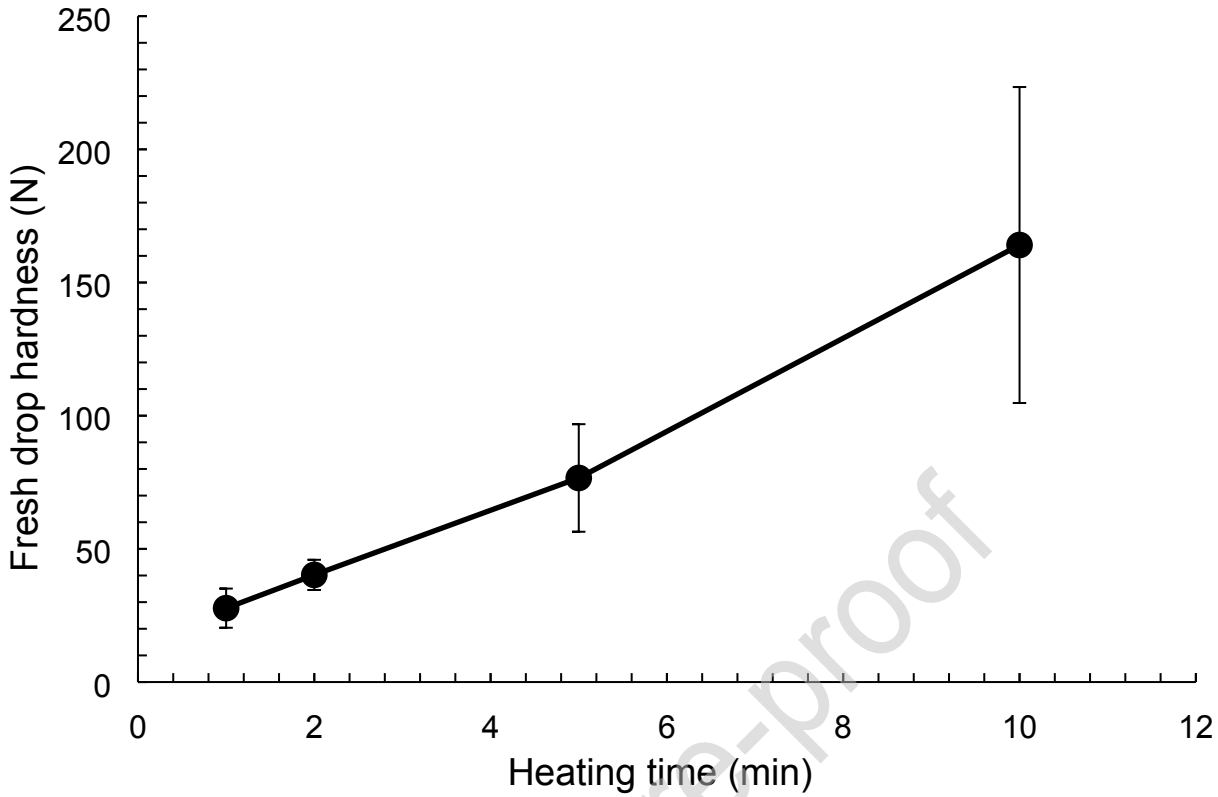

Figure 5. Effect of dehydration shown by heating time (min) at 100°C on the hardness (N) of drops comprised of 40% WPI with 10% sucrose; n = 3.

Journal Pre-proof

Journal Pre-proof

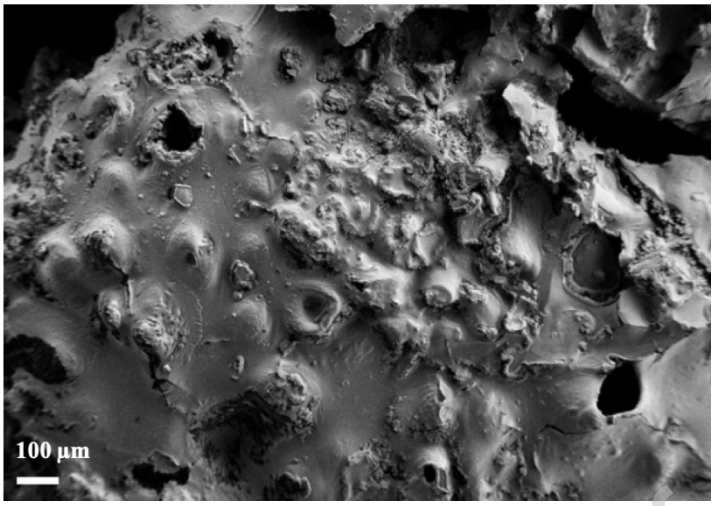

Figure 6a. Scanning electron micrograph image at 500x magnification, depicting the microstructure of a dried, 40% WPI bead.

Journal Pre-proof

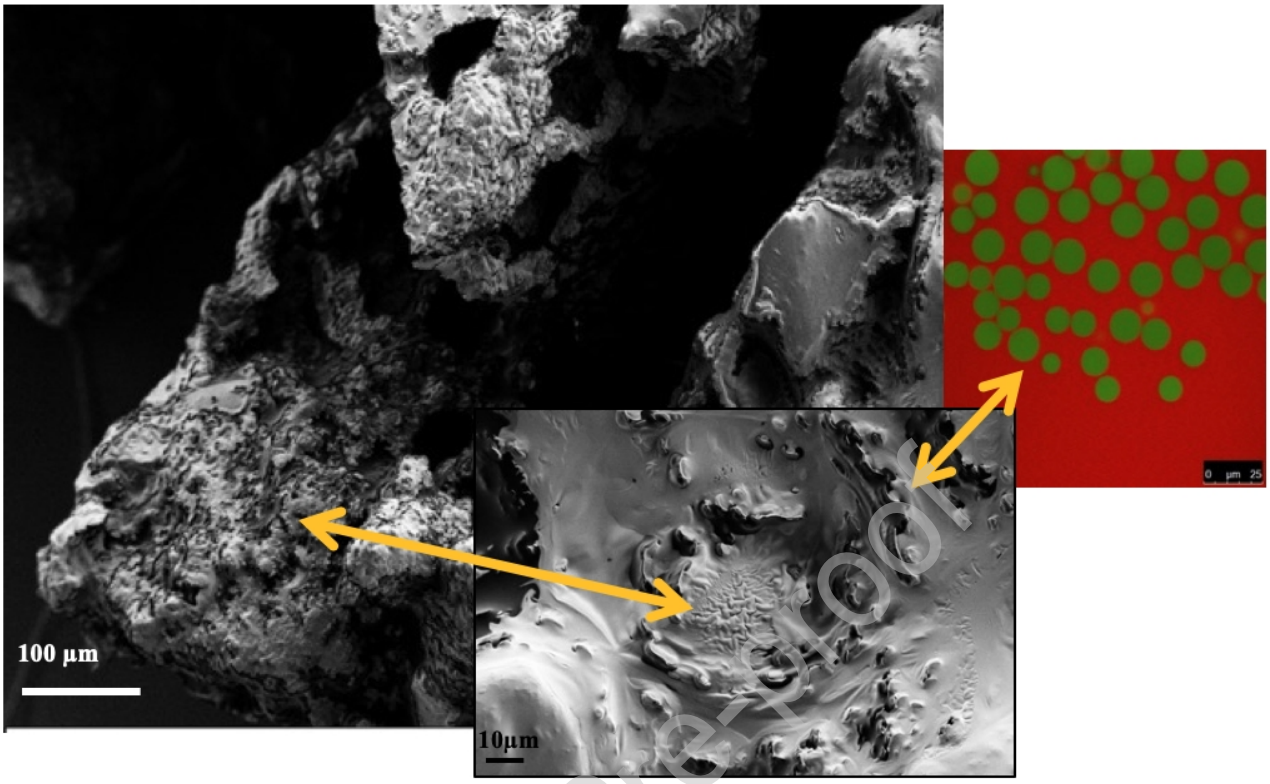

Figure 6b. Left: Scanning electron micrograph image at 1000x magnification, depicting the microstructure of a dried, 40% WPI bead. Center: Scanning electron micrograph image at 5000x magnification, depicting the microstructure of a dried, 40% WPI bead. Right: Confocal laser scanning micrograph image depicting the microstructure of a dried, 40% WPI bead, with oil droplets dispersed throughout image. The left arrow points towards the appearance of the protein network in the left and center images, and the right arrow highlights the oil droplets protruding throughout the structure in the center and right images. ***Color usage necessary***

Journal Pre-proof

Journal Pre-proof

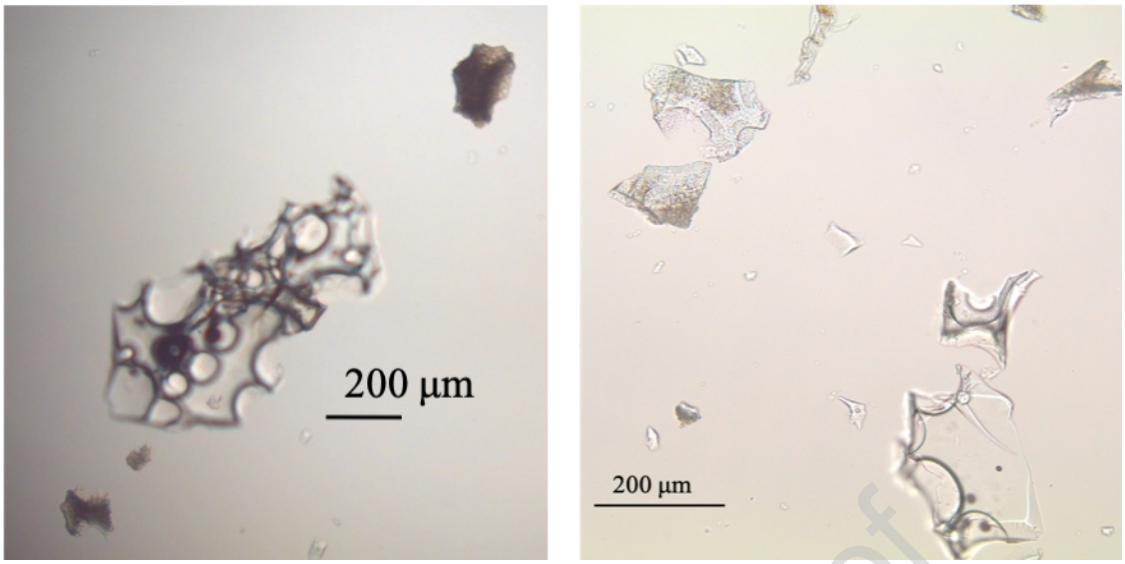

Figure 7a. Left: Optical light microscope image at 4x magnification, depicting the microstructure of a dried, 40% WPI with 10% sucrose bead. Right: Optical light microscope image at 10x magnification, depicting the microstructure of a dried, 40% WPI with 10% sucrose bead.

Journal Pre-proof

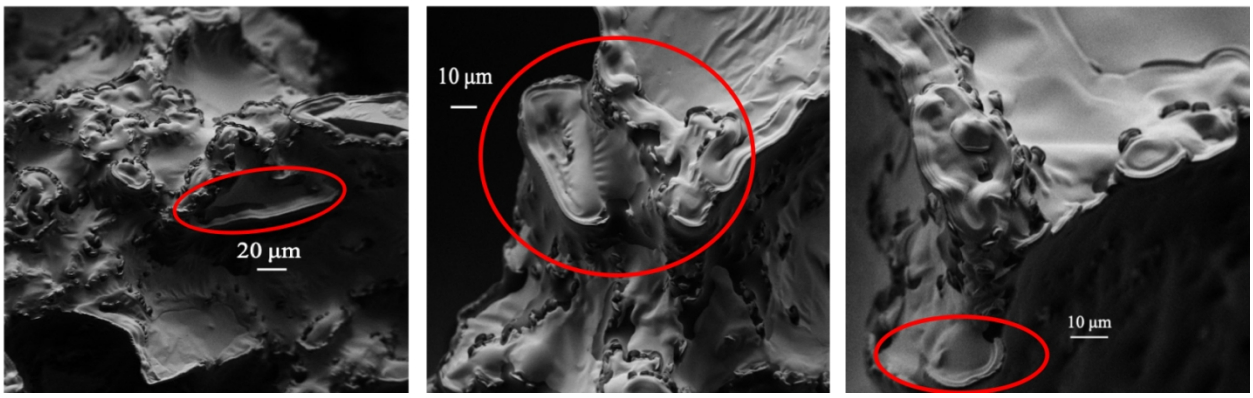

Figure 7b. Left: Scanning electron micrograph image at 500x magnification, depicting the microstructure of a dried, 40% WPI with 10% sucrose bead. Center: Scanning electron micrograph image at 1000x magnification, depicting the microstructure of a dried, 40% WPI with 10% sucrose bead. Right: Scanning electron micrograph image at 2000x magnification, depicting the microstructure of a dried, 40% WPI with 10% sucrose bead. ***Color usage necessary***

Journal Pre-proof

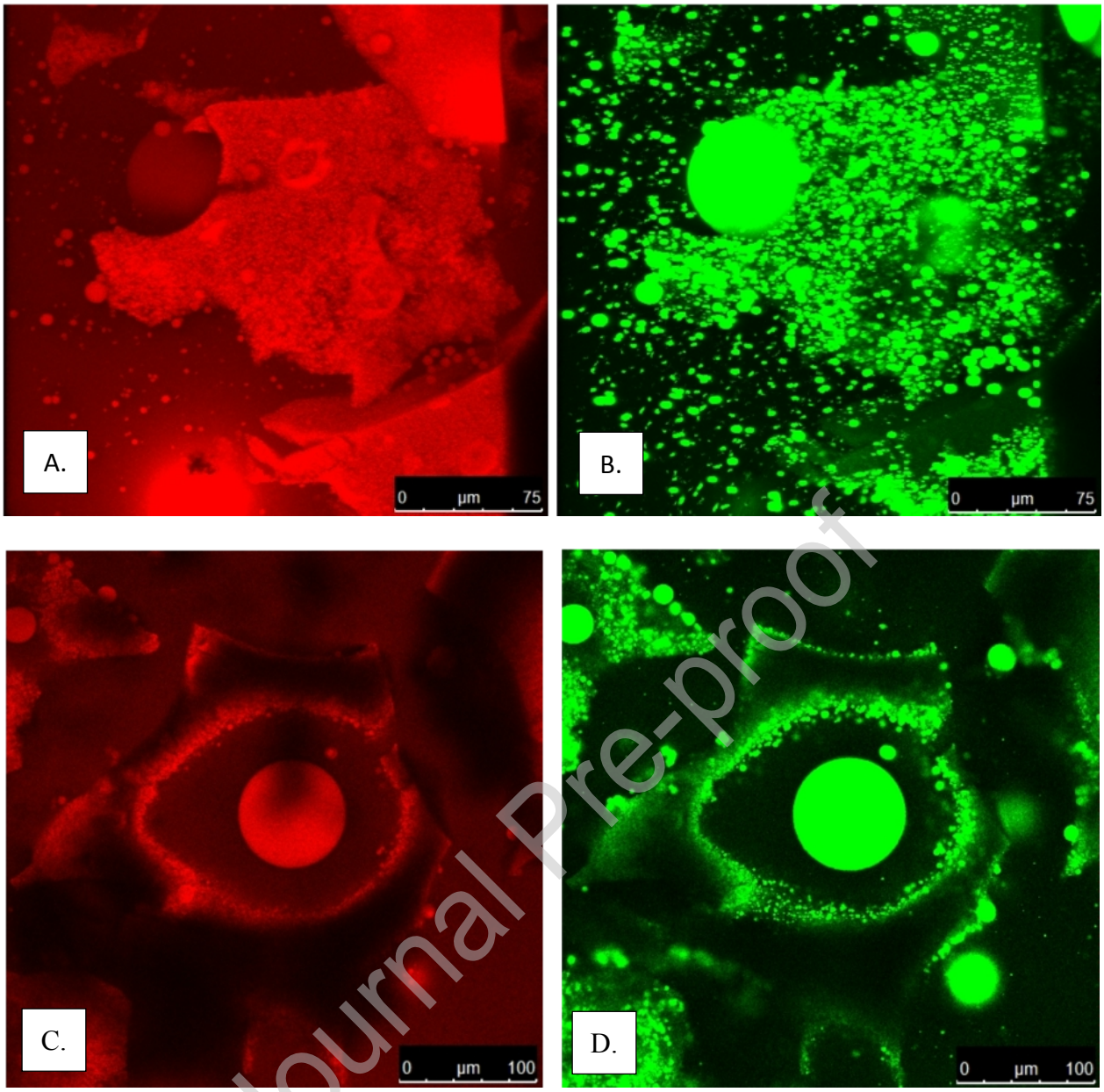

Journal Pre-proof

Figure 8 A-D. Confocal laser scanning micrograph images depicting the microstructure of a dried, 40% WPI with 10% sucrose bead, with oil droplets dispersed throughout image. A and C: Highlight protein in bright red and other components as darker colors. B and D: Highlight fat in bright green and other components as darker colors. ***Color usage necessary***

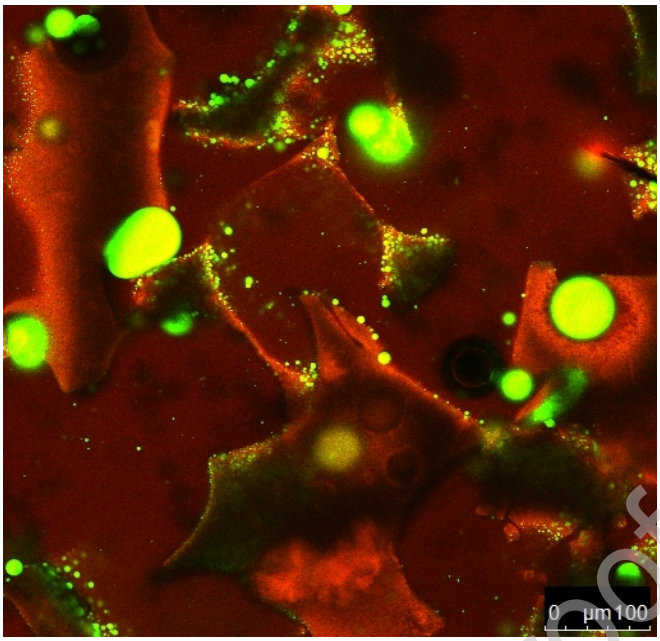

Figure 9. Confocal laser scanning micrograph image depicting the microstructure of a dried, 40% WPI with 10% sucrose bead, with oil droplets dispersed throughout image; highlighting proteins in bright red, fat in bright green, and other components (mainly sucrose) as darker colors. The darker colored sucrose is thought to form the translucent, glassy fragments shown throughout the image ***Color usage necessary***

Journal Pre-proof

Journal Pre-proof

Highlights

- Developed continuous process to transform concentrated protein-sucrose dispersion into solid beads
- Drops show rapid protein denaturation and gelation and water vaporization in heated oil bath, with simultaneous uptake of bulk oil into the structure and emulsification into small droplets
- Sucrose vitrifies to stabilize protein gel structure

Journal Pre-proof

Journal Pre-proof

Table 1. Feed formulations with WPI and sucrose concentrations (%) as well as pH.

[WPI]	[Sucrose]	pH
%		-
10	0	6.6
15	10	6.6
20	0	6.6
20	20	6.6
25	10	6.6
30	0	6.6
30	10	6.6
30	20	6.6
35	10	3.5, 4.0, 4.1, 4.2, 4.5, 5.0, 6.7
35	15	4.0, 4.5, 5.0, 6.6
35	20	4.5, 5.4, 6.6
40	0	6.6
40	5	6.6
40	10	4.5, 6.5

Journal Pre-proof

Journal Pre-proof

Table 2. Composition of liquid feeds chosen for bead formation

Liquid Feed Formulation	Water %	Total solids %	Protein (WPI) %	Sucrose %
30% WPI with 20% sucrose	50	50	30	20
35% WPI with 15% sucrose, pH 4.5	50	50	35	15
40% WPI	60	40	40	n/a
40% WPI with 10% sucrose	50	50	40	10

Journal Pre-proof

Journal Pre-proof

Table 3. Water activity (a_w) of intermediate, fresh beads prior to drying

Fresh Bead Formulation	a_w
30% WPI with 20% sucrose	0.91 ± 0.01
35% WPI with 15% sucrose, pH 4.5	0.91 ± 0.01
40% WPI	0.95 ± 0.01
40% WPI with 10% sucrose	0.90 ± 0.02

Journal Pre-proof

Journal Pre-proof

Table 4. Composition and a_w of final, dried beads

Dry Bead Formulation	a_w	Water %	[Solids + Oil] %
30% WPI with 20% sucrose	0.22 ± 0.05	2 ± 1	98 ± 1
35% WPI with 15% sucrose, pH 4.5	0.19 ± 0.03	1 ± 1	99 ± 1
40% WPI	0.20 ± 0.01	3 ± 1	97 ± 1
40% WPI with 10% sucrose	0.14 ± 0.02	1 ± 1	99 ± 1

Journal Pre-proof

Journal Pre-proof

Table 5. Total feed solids, viscosity, and surface tension data for feed dispersions that formed beads; n = 3

Feed	Total Solids (%)	Viscosity (Pa-s)	Surface tension (N/m)
40% WPI	40	0.51 ± 0.15	0.00186± 0.00006
40% WPI, 10% sucrose	50	1.73 ± 0.25	0.00205 ± 0.00003
30% WPI, 20% sucrose	50	0.34 ± 0.07	0.00156 ± 0.00009
35% WPI, 15% sucrose- pH 4.5	50	1.28 ± 0.03	0.00189 ± 0.00025

Journal Pre-proof

Table 6. Total volumes (cm^3) and true densities (g/cm^3) of dried drops comprised of 40% WPI with 10% sucrose (40/10) obtained at various heating times (min) at 100°C; values were used to calculate average total volumes and average solids volumes (cm^3), respectively, in order to calculate porosity (%).

Sample	Heating time at 100°C (min)	Total volume (cm^3)		Calculated average total volume (cm^3)	True density (g/cm^3)		Calculated average solids volume (cm^3)	Calculated Porosity (%)
		Rep 1	Rep 2		Rep 1	Rep 2		
40/10	1	3.90 ± 0.01	5.16 ± 0.02	4.53	1.11 ± 0.01	1.10 ± 0.01	2.61	42 ± 3[a]
40/10	2	3.86 ± 0.01	3.75 ± 0.01	3.80	1.07 ± 0.01	1.08 ± 0.01	2.27	41 ± 2[a]
40/10	5	4.09 ± 0.01	2.30 ± 0.02	3.19	0.99 ± 0.01	1.07 ± 0.01	2.09	34 ± 4[a]
40/10	10	2.65 ± 0.01	3.88 ± 0.01	3.26	1.07 ± 0.01	1.09± 0.01	2.02	38 ± 1[a]

Superscript letters in the same column indicate statistically significant ($p < 0.05$) difference

Journal Pre-proof